Journal of
Renewable Energy Research and Applications (RERA)

Vol. 6, No 1, 2024, 61-73 *DOI: 10.22044/rera.2024.13624.1251*

Lambert W Function-based Technique to Estimate and Compare Performance of Partially Shaded Series-parallel and Total-cross-tied Configured PV Array

A. Niti*

Shyamlal college, University of Delhi, India.

Received Date 18 September 2023; Revised Date 23 December 2023; Accepted Date 23 January 2023
Corresponding author: nitichin@yahoo.co.in (A. Niti)

Abstract
Partial shading condition (PSC) has a detrimental effect on the output performance of a photovoltaic (PV) system. The output performance of a partially shaded PV array depends not only on the pattern, intensity, and location of the shadow but also on its configuration. In this paper, the output performance of two configurations namely series-parallel (SP), a commonly used configuration, and total-cross-tied (TCT) have been compared under diverse PSCs. A Lambert W-function-based technique has been developed to model, simulate, and estimate the performance of both the configurations of the PV array. The developed program can evaluate the current, voltage, and power for the arrays of different sizes under uniform and different PSCs. A detailed investigation has been carried out for the output performance of both the configurations under nine diverse shading patterns and different sizes of the arrays. Comparative analysis for the configurations is presented based on parameters such as maximum power obtained, partial shading power loss percentage, efficiency, and fill factor. It has been found from the obtained results that output performance of a PV array under PSC is enhanced by using TCT configuration compared to SP configuration.

Keywords: *Partial shading. Lambert W-function, Series-parallel, Total-cross-tied, Power loss.*

1. Introduction

In the current global scenario, the gap between demand and supply of energy is continually increasing. Solar photovoltaic (PV) is a potential source, which can provide the long-term sustainable solution to the energy crisis, which the world is witnessing today. Solar cell is the basic photovoltaic device, which converts sunlight into electricity. For the desired outdoor energy generation, clusters of solar cells are interconnected to form the PV module, which are further interconnected to form PV arrays.

A PV solar cell can be represented either by the single diode model [1, 2] or double diode model [3, 4]. Single diode model is widely used because it is a simple and accurate model, consisting of five parameters [1, 5]. These five parameters are-ideality factor, series resistance, shunt resistance, photo current, and saturation current. Several types of methods such as numerical and analytical, have been proposed by the researchers to evaluate the model parameters [6-11]. Numerical methods are dependent on the initial values chosen and sometimes there may be convergence issues. Analytical methods express the PV I-V transcendental equation explicitly. Analytical method is faster and has a better accuracy in comparison to numerical methods [10, 11]. Lambert W function is a valuable tool, as it solves the transcendental I-V equation of the solar cell/module [12-14]. Using Lambert W function, the PV current is obtained in terms of PV voltage (and vice versa) explicitly, thus bringing along computational advantage in terms of accuracy and time [11, 15, 16]. Many researchers have used Lambert W function for different applications, e.g. the authors of [17] presented an exact explicit solution based on the Lambert W-function to calculate the optimum load of an illuminated solar cell containing a parasitic series resistance and a shunt resistance. In [18] an optimized technique, using Lambert W-function and polynomial curve fitting method to describe the I-V and P-V characteristics of solar cell, and module was presented. Cubas *et al*. presented a method based on analytical formulation, which turns the series resistor equation explicitly by using Lambert W

function [19]. The expression was used to analyse performance of two commercial solar panel at different values of irradiation and temperature. Tripathy *et al*. modelled a PV system using Lambert W function technique [20]. The model was simulated under sunny and cloudy day condition. Authors found that the Lambert W function-based mathematical model was accurate and achieved good agreement between calculated and simulated outputs. Li *et al*. reduced the explicit equation of the single diode model expressed by the Lambert W function to its simplified form [21]. To estimate the model parameters of solar cells and PV modules, the authors combined the simplified explicit equation with an intelligent optimization algorithm. The accuracy of parameter extraction was improved, and also the robustness and convergence speed were increased.

For the field installed PV arrays, partial shading condition (PSC) or the condition where the irradiance received by the entire PV array is not uniform, is a huge challenge. This type of condition is commonly confronted by the installed PV array because of the presence of any nearby structure like building or tree or due to accumulation of dust, fallen leaves, bird droppings, etc. Partial shading of solar panels results in mismatching power loss [22-25]. Hence, the efficiency and capacity of a PV system to generate maximum power is reduced. Bastidas *et al*. presented a model for photovoltaic fields and a procedure for calculating the parameters of the PV modules of a string (PV modules connected in series) [26]. By using the Lambert-W function, the string voltage was expressed as an explicit function of the load current. Batzelis and Routsolias also presented a PV string model, where the terminal voltage was expressed as an explicit function of the current using Lambert W function, resulting in significantly reduced calculation times and improved robustness of simulation [27]. Simplified formulae were also presented, which can calculate the maximum power points of a PV string operating under PSCs. In [28], a technique for tracking the MPP of PV modules connected in series, parallel and series-parallel configurations under shading effect was proposed. The author used the Lambert W function to express the output characteristics of various configured PV modules. The obtained equations were converted into the discrete form, and the maximum output power of each configuration was calculated by numerically solving the discrete equations. In [29], the comparative effect of partial shading on series and parallel configuration of PV array using Lambert W-function was presented. These previous studies employing Lambert W function are limited to only series, parallel and series-parallel configuration under the impact of PSCs. In an effort to alleviate power loss due to shading, the researchers have tried different configurations and reconfiguration of PV array [30-43]. In open literature, different configurations such as honey comb, bridge linked, and total cross tied are present [36-37, 39]. Researchers have tested these configurations using different methodologies to find the configuration least susceptible to power loss under PSC, e.g. simulation studies based on computational network analysis approach [33], solving the simultaneous nonlinear equations using Newton Raphson algorithm [34], developing Matlab M-code based on numerical method techniques [35]. These methods are either computationally complex or convergence can become an issue when obtaining numerical solution for large system of equations. Studies based on simulation using MATLAB/SIMULINK platform [30, 32, 35] and few experimental studies [41-43] have also been conducted in this regard. Study of effect of PSC on PV array in real field conditions is expensive, needs lot of time, and depends strongly on the existing weather conditions. In addition, for a comparative study of different configuration, it is not possible to maintain same natural shading pattern on different arrays throughout the experiment in field conditions. Studies based on simulation work are easier to conduct. However, study of different configurations of PV array using Lambert W function under PSC is still lacking.

As presented in the literature survey, Lambert W is a strong tool, which can express PV I-V equation explicitly with better accuracy. However, its application to model and simulate the performance of different PV array configurations is still lacking. This has motivated the author to develop a method based on Lambert W-function to simulate the output performance of different PV array configurations under PSCs. The present work would be beneficial for researchers/ engineers/solar project developers in gaining knowledge of performance of PV array in field conditions by reproducing their behaviour for any working condition. The results of this work are also significant in developing future technique for power loss minimization.

In the present work, a technique based on Lambert W-function has been developed to simulate the output performance of Series-parallel (SP) and Total cross tied (TCT) PV array configurations

under uniform as well as partial shaded conditions. Comparative analysis for SP and TCT configuration on the basis of maximum power was obtained; partial shading power loss percentage, efficiency, and fill factor is presented thereafter. For this study, the MATLAB software has been used to develop programs for evaluating the current, voltage, and power for both the arrays. The core of the programs essentially comprises of determining explicitly I-V relation for each PV module using Lambert W-function. The detailed flowchart of the algorithm is presented in Section 4.

The structure of this research paper is as follows: Section 2 presents the mathematical modelling of PV module, Section 3 describes the mathematical modelling of a string of PV modules connected with bypass diodes; Section 4 presents the modelling and simulation of PV arrays using the method developed. Section 5 presents output performance analysis of SP and TCT configured PV array, Conclusions are drawn in Section 6.

2. Modelling of PV module using Lambert W-function

Solar cell is extensively represented by the single diode model owing to its simplicity (Fig. 1) [1, 5]. On the bases of this model, the current-voltage characteristic of a PV module having N_s solar cells in series is obtained by (1) [26].

$$\mathbf{I_m = I_{ph} - I_o \left[\exp\left(\frac{V_m + I_m R_s N_s}{n V_{th} N_s}\right) - 1\right] - \left(\frac{V_m + I_m R_s N_s}{R_{sh} N_s}\right)} \quad (1)$$

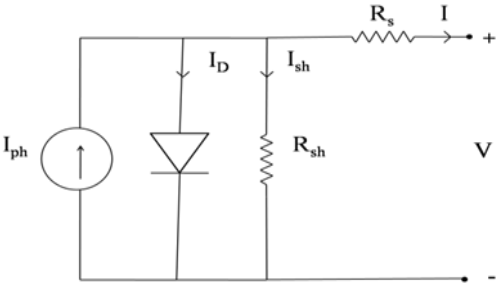

Figure 1. Single diode model of a solar cell.

Using Lambert W-function, the explicit solution of transcendental current-voltage equation of PV module is obtained by (2).

$$\mathbf{V_m = I_o R_{sh} N_s + I_{ph} R_{sh} N_s - I_m R_s N_s - I_m R_{sh} N_s - n N_s V_{th} LambertW\left(\left(\frac{R_{sh} I_o}{n V_{th}}\right) e^{\left[\frac{(I_o + I_{ph} - I_m) R_{sh}}{n N_s V_{th}}\right]}\right)} \quad (2)$$

For any module temperature T and solar irradiation G, the photo-generated current of the module is given by (3) [1].

$$\mathbf{I_{ph} = \left[I_{phn} + K_I (T - T_n)\right]\left(\frac{G}{G_n}\right)} \quad (3)$$

The short-circuit current of the PV module using Lambert W function is obtained by (4).

$$I_{sc} = \frac{R_{sh}(I_o + I_{ph})}{R_s + R_{sh}} - \frac{(n V_{th})}{R_s} * \text{Lambert W}\left[\exp\left[\frac{R_{sh} I_o R_s N_s}{(R_s + R_{sh}) n N_s V_{th}}\right]\right] \quad (4)$$

3. Modelling of PV module string with by-pass diodes

A PV string is a cluster of PV modules connected in series. When a PV string is partially shaded, even the fully illuminated modules are forced to operate at lower current dictated by the short circuit current of the most shaded module ($I_{SC,msh}$) in the string. This results in huge loss in the output power. This power loss is minimized to an extent by incorporating bypass diodes in parallel to the module, as shown in figure 2.

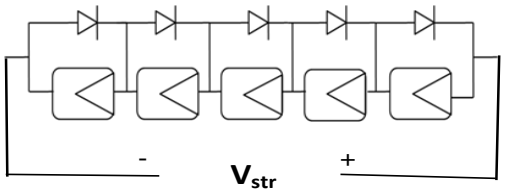

Figure 2. A string of PV modules with by-pass diodes connected in parallel.

In the absence of partial shading, the bypass diode remains in the non-conducting state. Under partial shading, the shaded module become reverse biased and the negative voltage developed across the module makes the bypass diode forward biased [27]. The diode then conducts the difference between the string current (I_{str}) and $I_{SC,msh}$. Hence, for any string current, voltage across any module (V_m) is calculated as follows:

If $I_{str} \leq I_{SC,msh}$, by-pass diode is in OFF state. V_m is given by (2).

If $I_{str} > I_{SC,msh}$, by-pass diode is in ON state. V_m is equal to the forward voltage drop across the bypass diode, given by (5) [27].

$$\mathbf{V_m = -a_{bd} . ln\left(\frac{I_{str} - I_{SC,msh}}{I_{sbd}} + 1\right)} \quad (5)$$

Voltage across the complete string (V_{str}) is equal to the sum of voltages of all the individual modules connected in that string.

$$\mathbf{V_{str} = \sum V_m} \quad (6)$$

4. Modelling and simulation of PV array configurations

In this section, a brief review of Series-parallel (SP) and Total cross-tied (TCT) configuration of PV array is presented, followed by the flowchart of the programs used to simulate their output performance under unshaded and shaded conditions.

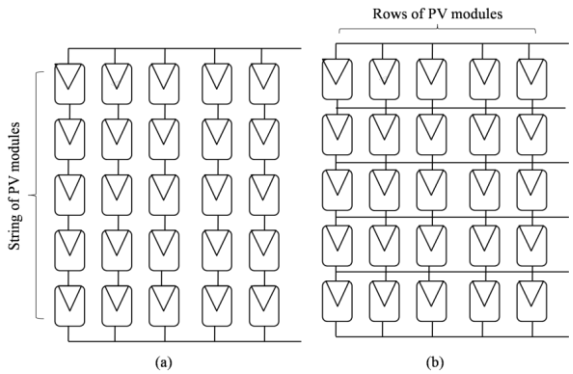

Figure 3. Schematic representation of PV array configurations (a) SP (b) TCT.

4.1. Series-parallel (SP) PV array configuration

To form the series-parallel array configuration, the modules are first connected in series to form series string, and then these strings are connected in parallel, as shown in figure 3(a). Array current (I_a) is equal to the sum of currents of individual strings. Array voltage (V_a) is equal to the voltage across any string.

$$\mathbf{I_a} = \sum \mathbf{I_{str}} \tag{7a}$$

$$\mathbf{V_a} = \mathbf{V_{str}} \tag{7b}$$

This configuration is widely used owing to its simplicity and ease of construction. Fig. 4a shows the flowchart to simulate the output characteristics of SP configured PV array. One by-pass diode per module in the array has been considered in this work.

4.2. Total-cross-tied (TCT) PV array configuration

Total cross-tied array configuration is a derivative of series-parallel configuration. When ties are connected across each row of junction TCT configuration is obtained, as shown in figure 3(b) [33]. In this configuration, all the modules in a row are connected in parallel. Several such rows are then connected in series. For any row, current (I_{row}) is equal to the sum of currents of all the modules in it, and voltage (V_{row}) is equivalent to voltage across any module in a row. Array current is equivalent to any row current. Array voltage is equal to the sum of voltages across each row.

$$\mathbf{I_a} = \mathbf{I_{row}} \tag{8a}$$

$$\mathbf{V_a} = \sum \mathbf{V_{row}} \tag{8b}$$

figure 4a and 4b present the flowchart to simulate the output characteristics of SP and TCT configured PV array respectively. In this work, one by-pass diode per module in the array has been considered.

4.3. Shading patterns used

For this study, nine random different shading patterns (shd-1 – shd-9) are used, as illustrated in figure 5. Shd-0 represents the case of no shading with uniform irradiance of 1000 W/m^2 falling on PV array. Array size used for this investigation is 5X5.

Next, the impact of same shadow pattern on SP and TCT arrays of different sizes-3 x 3, 3 x 4, 4 x 3, as illustrated in Figure 6, has been investigated.

The purpose of this part of the study is to investigate the role of array size on its output performance in terms of maximum power obtained, partial shading, efficiency, and fill factor, and to draw a comparison between both the configurations.

4.4. Performance parameters of SP and TCT configured PV array

For this study, parameters of KYOCERA KC200GT PV module (given in Appendix A.1.) has been used for simulation. Size of the array used is 5 x 5. One by-pass diode per module in the array has been considered. The comparative performance analysis of SP and TCT PV arrays under PSCs has been conducted in terms of maximum power obtained, partial shading power loss percentage, efficiency, and fill factor.

The partial shading power loss of the PV array (ΔP_{PS}) is given by equation (9).

$$\Delta \mathbf{P_{PS}}(\%) = \left(\frac{\mathbf{P_{Max}} - \mathbf{P_{shd}}}{\mathbf{P_{Max}}}\right) \times \mathbf{100} \tag{9}$$

Fill factor (FF), an indicative of the performance of PV array, is given by equation (10).

$$\mathbf{FF} = \frac{\mathbf{V_{mp}} \times \mathbf{I_{mp}}}{\mathbf{V_{OC}} \times \mathbf{I_{SC}}} \tag{10}$$

Efficiency (η) is the ratio of the maximum output power generated by the PV array to the input power from sun and is calculated using equation (11).

$$\boldsymbol{\eta}\ (\%) = \frac{\mathbf{V_{mp}} \times \mathbf{I_{mp}}}{\mathbf{G} \times \mathbf{A}} \times \mathbf{100} \tag{11}$$

where 'G' is the input solar irradiance per unit area (W/m^2) and 'A' is the area of the PV array on which it falls.

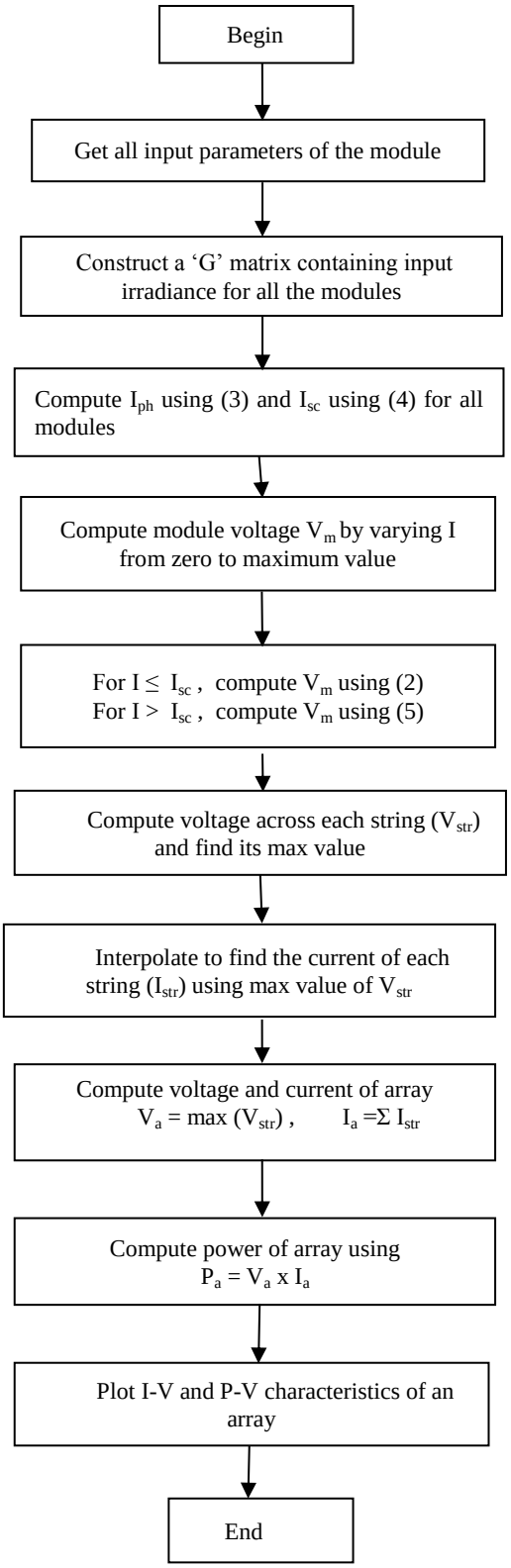

(a)

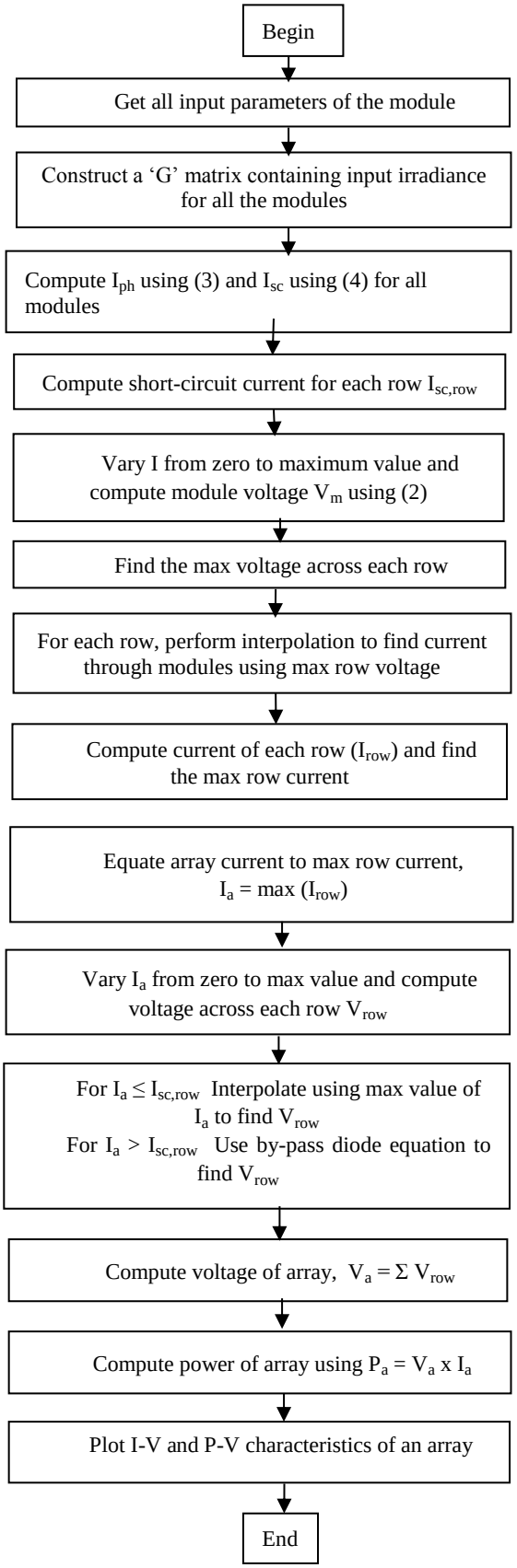

(b)

Figure 4. Flowchart to simulate the output characteristics of (a) SP (b) TCT PV array.

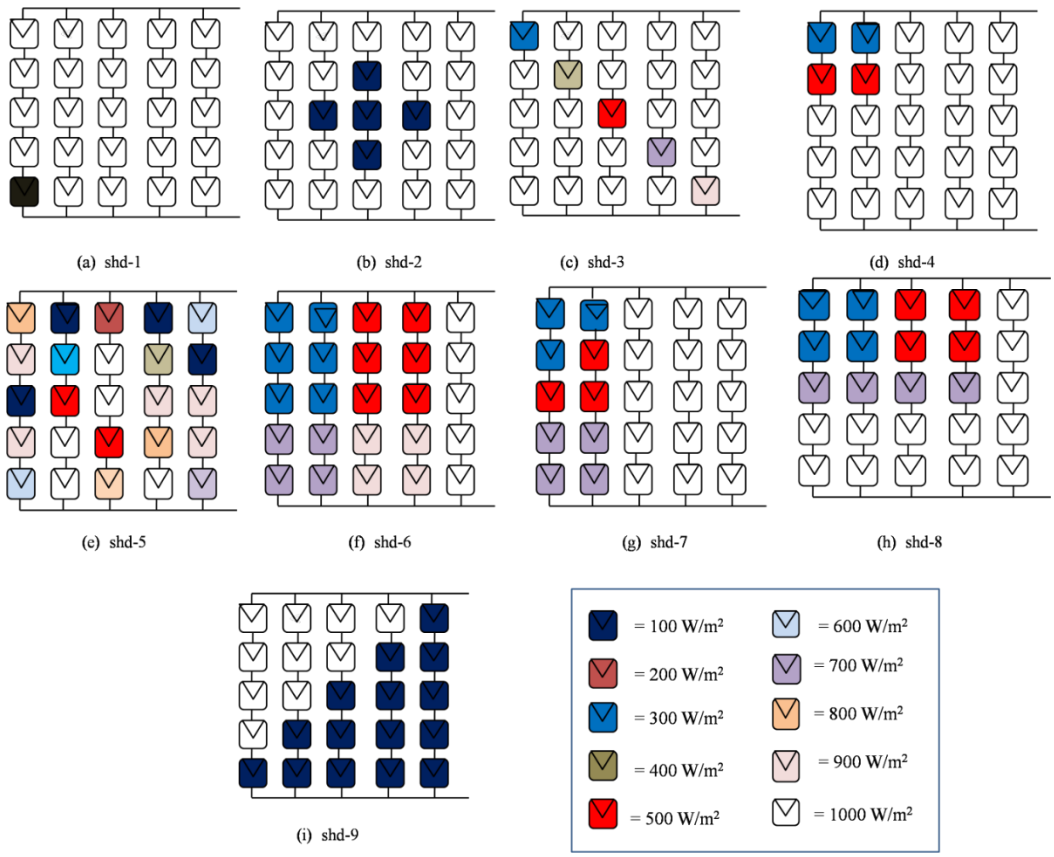

Figure 5. Illustration of different shading patterns.

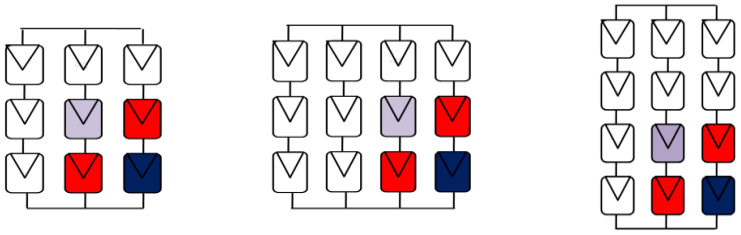

(a) 3X3 **(b) 3X4** **(c) 4X3**

Figure 6. Different array sizes with same shading pattern.

4.5. Validation of the proposed technique

To validate the proposed method, the output power, efficiency (%) and fill factor of SP and TCT configured PV array under different PSCs reported in a previous work [30] has been estimated using the present method and is presented in table 1. The obtained results are in close agreement with the previous results.

Table 1. Parameters of partially shaded SP and TCT array configuration reported in Ref. [30] and obtained using the present method.

Shading case	Max. power (W)		Efficiency (%)		Fill factor	
			SP configuration			
	Ref. [30]	Present method	Ref. [30]	Present method	Ref. [30]	Present method
Uneven column shading	4296.4	4325.1	13.38	13.47	0.681	0.685
Uneven row shading	3939.3	3961.1	12.27	12.34	0.588	0.591
Short & wide shading	2725.4	2732.4	10.14	10.27	0.406	0.412
			TCT configuration			
Uneven column shading	4490.9	4489.4	13.99	13.98	0.713	0.711
Uneven row shading	3970.0	3958.3	12.37	12.33	0.592	0.591
Short & wide shading	2862.9	2851.0	10.66	10.72	0.432	0.430

5. Results and discussion

5.1. Under uniform irradiance

The obtained output I-V and P-V characteristics of SP and TCT configuration under uniform irradiance is presented in figure 7. Both the configurations display a single power peak in their P-V characteristics and generate same maximum output power of 5000.5 W.

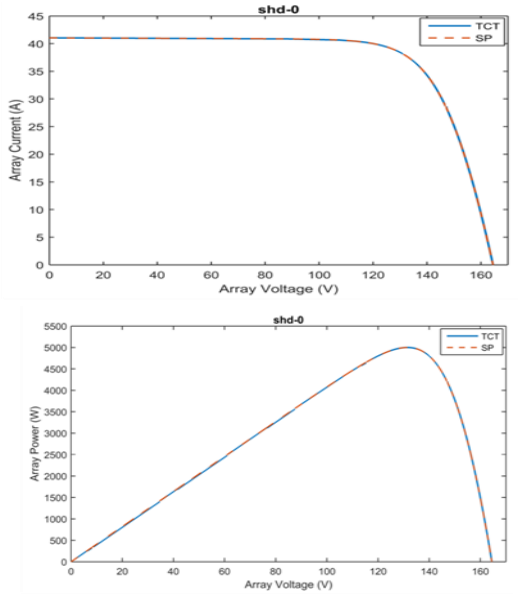

Figure 7. I-V and P-V characteristics of SP and TCT configured arrays under uniform irradiance of 1000 (W/m^2).

5.2. Impact of different shading patterns on arrays of same size

Simulated output I-V and P-V characteristics under different shading patterns for SP and TCT configurations are shown in figures 8 and 9, respectively. Under PSC, the output P-V characteristic exhibits more than one power peak. The number of power peaks appearing in the output characteristics depends on the shading pattern.

Simulated values of maximum output power, efficiency, and fill factor for SP and TCT configurations is presented in table 2. Among all the shading patterns considered, maximum power is generated by both SP and TCT configurations under shd-1. SP configuration generated 4421.1 W, while TCT generated 4512.8 W. Only one shaded module, receiving 100W/m^2 irradiance, in the array resulted in a power loss of 11.59% in SP and 9.75% in case of TCT configuration. This type of small-localized shading can commonly occur due to fallen leaf or bird dropping on the PV panel. Least power is generated by both the configuration under shd-9 under, which 15 modules in the array received only 100W/m^2 irradiance. However, TCT still generated 46.5 W more than SP configuration.

Table 2. Simulated values of various parameters of SP and TCT array configuration under different shading patterns.

Shading case	SP PV array			TCT PV array		
	Max. power (W)	Efficiency (%)	Fill factor	Max. power (W)	Efficiency (%)	Fill factor
Shd-0	5000.5	14.14	0.74	5000.5	14.14	0.74
Shd-1	4421.1	12.97	0.66	4512.8	13.24	0.70
Shd-2	3411.4	11.77	0.51	3415.6	11.78	0.51
Shd-3	3960.2	12.28	0.59	4488.4	13.92	0.68
Shd-4	3726.4	11.66	0.56	4003.6	12.53	0.60
Shd-5	2264.1	9.95	0.36	2372.3	10.42	0.44
Shd-6	2679.4	11.70	0.49	2733.2	11.93	0.50
Shd-7	3642.5	12.74	0.62	3857.3	13.50	0.66
Shd-8	2741.2	10.21	0.41	2862.1	10.65	0.43
Shd-9	1423.7	8.76	0.28	1470.2	9.04	0.28

Under both shd-5 and shd-6, though 80% of the array is shaded, but the shadow distribution over the array surface is different. It has been observed that the individual output power of both the configurations obtained under these two shading scenarios is very different (2372.3W, 2733.2W for TCT; 2264.1W, 2679.4W for SP for shd-5 and shd-6, respectively). TCT still generated more power than SP under both the shading patterns.

On the other hand, under shd-6 and shd-8 the arrays are 80% and 48% shaded respectively yet the output power obtained for any array is not very different from each other (2733.2 W, 2862.1 W for TCT; 2679.4 W, 2741.2 W for SP for shd-6 and shd-8 respectively). As is evident, TCT generated more power than SP in these cases also. SP configuration's obtained maximum efficiency and fill factor is 14.14% and 0.66, which is

increased to 13.24% and 0.70, respectively, for TCT configuration under shd-1. Under shd-9, both SP and TCT exhibited least efficiency and fill factor (8.76% and 0.28 for SP; 9.04% and 0.28 for TCT). In comparison to SP, TCT output performance is marginally improved under shd-9. In general, efficiency and fill factor of TCT configuration is better than SP under different shading cases.

The power loss incurred by both the PV array configurations under different shading cases is presented in figure 10. The results clearly demonstrate that TCT configured PV array suffers less power loss than SP under different PSCs.

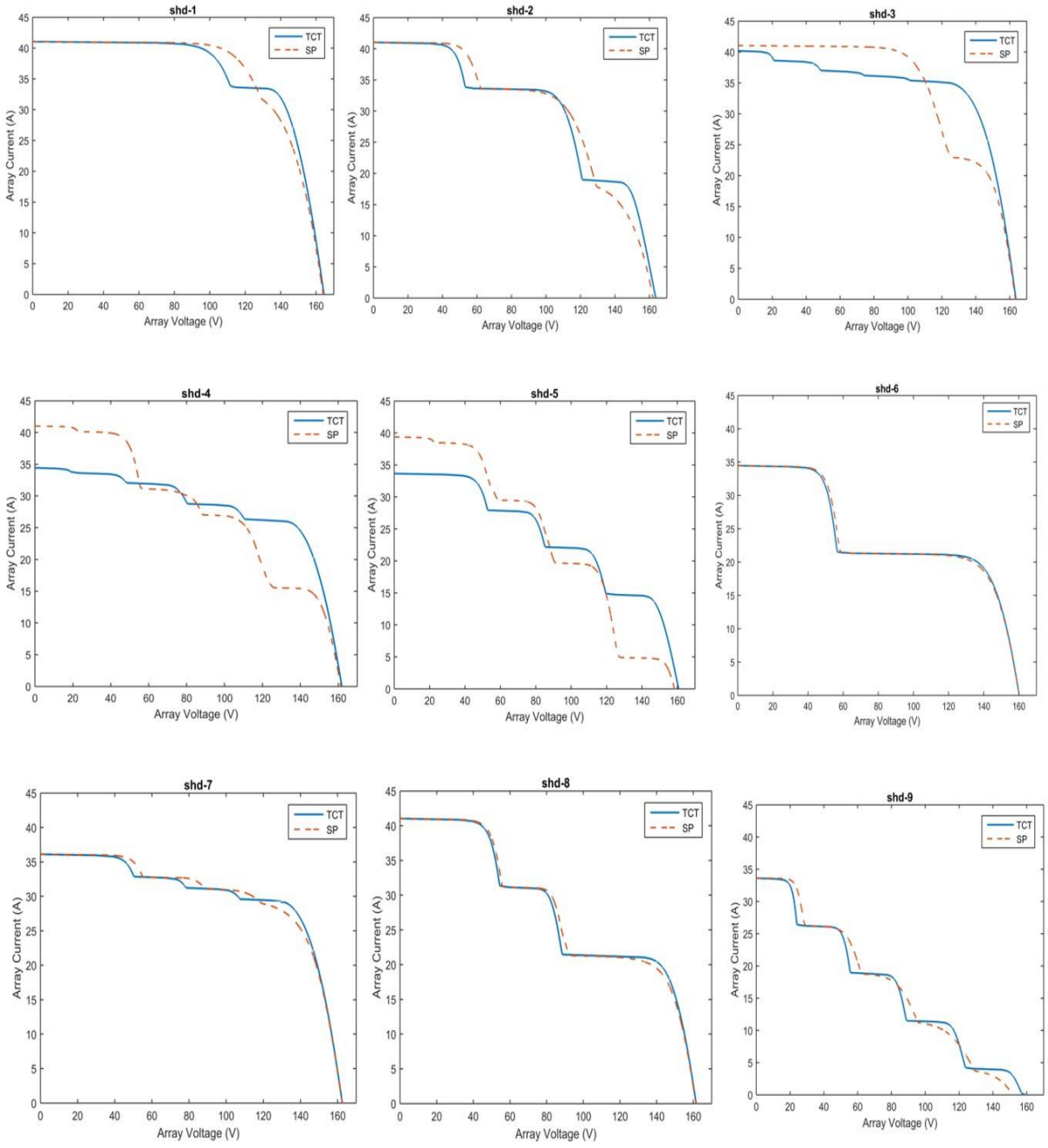

Figure 8. I-V output characteristics of SP and TCT configured arrays under different shading patterns.

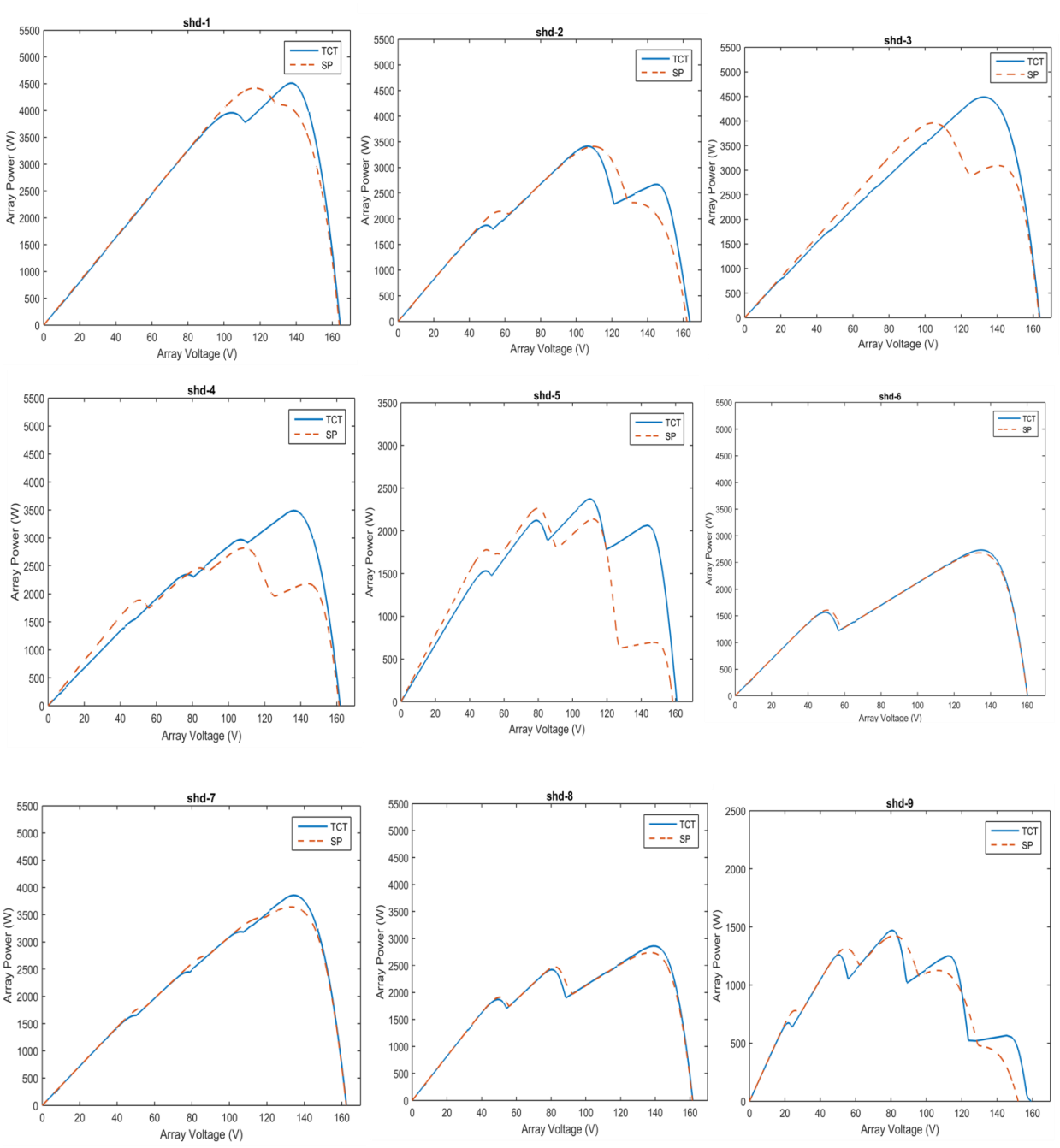

Figure 9. P-V output characteristics of SP and TCT configured arrays under different shading patterns.

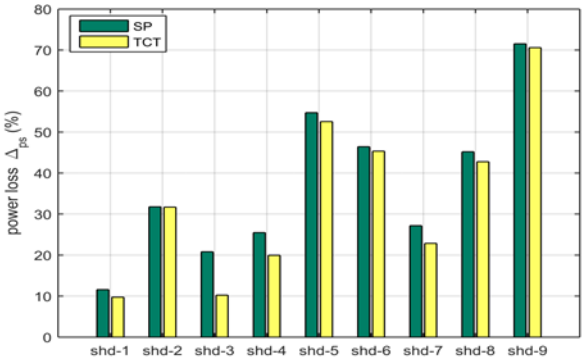

Figure 10. Partial shading power loss (%) for SP and TCT configured PV array under different shading scenarios.

5.2. Impact of same shading pattern on different-sized arrays

The simulated results for different sized SP and TCT configurations of PV array under the impact of same shading pattern is presented in table 3. The results clearly demonstrate that for all array sizes under constant shading pattern, TCT configured PV array exhibits superior performance than SP. For the array size 3 X 3, power generated by the SP configuration is 1120.9 W, which in case of TCT is increased to 1180.01 W. Considering 3 X 3 as the base size, it is observed that the impact of the addition of one column (array size-3X4) on the output

performance of PV array is different from the impact of the addition of one row (array size-4X3). The output power of 3 X 4 SP configured array is 596.5W more than 3 X 3 sized array, an increase of 53.2%. In case of TCT, it is 632.8W, an increase of 53.6%. The output power of 4 X 3 SP configured array is 379W more than 3 X 3 sized array, an increase of 33.8%. In case of TCT, it is 433.9 W, an increase of 36.8%. For both the configurations, efficiency and fill factor in case of 3 X 4 size is more than 4 X 3.

Array size	SP PV array			TCT PV array		
	Max. power (W)	Efficiency(%)	Fill factor	Max. power (W)	Efficiency (%)	Fill factor
3X3	1120.9	11.33	0.47	1180.1	11.92	0.49
3X4	1717.4	12.14	0.54	1812.9	12.82	0.57
4X3	1499.9	10.60	0.47	1614.0	11.41	0.50

It is inferred from the obtained results that for any configuration, power loss due to partial shading cannot be determined in a direct way as it is not proportional to the shaded area but depends on the pattern, distribution, intensity of the shade, and its configuration. However, under PSCs, PV array with TCT configuration is less susceptible to power loss than SP configuration. This is due to the presence of a greater number of cross ties in TCT configuration, which provide more current paths. Therefore, even when the current is reduced in other branches due to PSC, the total current restriction is prevented due to the presence of alternate current paths. This makes the configuration more reliable in case of PSCs or interconnection fault. For a large-scale PV system, though SP is a simpler configuration to implement, its performance is inferior to TCT under PSCs. On the other hand, implementation of TCT configuration in a large-scale PV system can increase the complexity due to the presence of larger number of ties. However, TCT is more partial shading tolerant in comparison to SP Repeated partial shadings can result in significant loss in the annual energy yield the of PV array [44, 45]. Therefore, to get the required energy yield, installation of more PV modules would be needed, which implies higher cost of electricity for the end users. Therefore, implementing TCT configuration can minimize the loss of energy yield, especially under repeated PSCs, benefitting the consumers as well as solar project developers.
The program developed in the present work is based on the single diode model of PV cell and Lambert W function. A comparison of programs to simulate the output performance of different arrays under PSC based on single diode and double diode model of PV cell needs to be done in terms of accuracy, complexity and speed, which is the scope of the author's future work.

6. Conclusions

Comparison of output performance of SP and TCT configured PV arrays under the impact of PSC by developing a Lambert W function-based technique has been presented. Using this technique, output I-V and P-V characteristics of both the array configuration have been obtained under diverse shading patterns and different array sizes. Maximum output power, partial shading power loss (%), efficiency, and fill factor for both the configurations have been estimated. After analyzing the performance of both the configurations, it is concluded that under PSCs performance of TCT configuration excels over SP. Therefore, mitigation of power loss and performance enhancement of PV system under PSCs can be achieved using TCT configured PV array instead of commonly used SP array configuration. The program developed for conducting this study is a user friendly and reliable method, which can be used to simulate performance of arrays of different sizes under uniform irradiance condition and different shading patterns. The insight provided by this research work will contribute to future technique development for power losses minimization.

7. Nomenclature

G	Solar irradiance (W/m^2)
G_n	Solar irradiance at STC (W/m^2)
I_a	PV array current (A)
I_m	PV module current (A)
I_{mp}	PV array current at maximum power point (A)
I_o	Reverse saturation current (A)
I_{ph}	Photo-generated current by PV module (A)
I_{phn}	Photo-generated current by PV module at nominal STC (A)
I_{row}	Current in row of parallel connected PV modules (A)
$I_{sc,row}$	Short circuit current of row of parallel connected PV modules (A)
I_{sbp}	By-pass diode coefficient (A)

I_{sc}	Short circuit current of PV module (A)
$I_{sc,msc}$	Short circuit current of most shaded module in a string of PV modules (A)
I_{str}	Current of string of PV modules (A)
K_I	Current/temperature coefficient of PV module (A/K)
N_s	Number of solar cells in series in a PV module
P_a	PV array power (W)
P_{max}	Maximum power generated by PV array at STC (W)
P_{shd}	Maximum power generated by shaded PV array (W)
R_s	Series resistance of solar cell (Ω)
R_{sh}	Shunt resistance of solar cell (Ω)
T	Temperature of the PV module (K)
T_n	Temperature of the PV module at STC (K)
V_a	PV array voltage (V)
V_m	PV module voltage (V)
V_{mp}	PV array voltage at maximum power point (V)
V_{oc}	Open-circuit voltage of PV module (V)
V_{str}	Voltage across string of PV modules (V)
V_{row}	Voltage across row of parallel connected PV modules (V)
V_{th}	Thermal voltage (= kT/q) of solar cell (V)
a_{bp}	By-pass diode coefficient (V)
k	Boltzmann's constant
n	Diode ideality factor
q	Charge of the electron

8. Appendix A

Parameters of KYOCERA KC200GT PV module used for simulation are given in table A1.

Table A.1 Parameters of KYOCERA KC200GT PV module.

S. No.	Parameters	values
1	Maximum power, P_{max}	200.143 W
2	Voltage at maximum power, V_{mp}	26.3 V
3	Current at maximum power, I_{mp}	7.61 A
4	Open-circuit voltage, V_{oc}	32.9 V
5	Short-circuit current, I_{sc}	8.21 A
6	Temperature coefficient of open circuit voltage, K_V	-0.1230 V/K
7	Temperature coefficient of short circuit current, K_I	0.0032 A/K
8	Series resistance, Rs	0.2318 Ω
9	Shunt resistance, Rsh	603.4349 Ω
10	Diode ideality factor, n	1.3
11	Number of cells per module,N_S	54
12	Area of PV module	(56.2 X 39.0) sq. in.

9. References

[1] Villalva, M.G. (2009). Comprehensive approach to modelling and simulation of photovoltaic arrays. IEEE Transactions on Power Electronics, Vol. 24, pp. 1198-1208.

[2] Datta S.K, Mukhopadhyay K., Bandopadhyay S., and Saha H. (1992). An improved technique for the determination of solar cell parameters. Solid-State Electronics, 35: 1667-1673.

[3] Sulyok, G. and Summhammer, J. (2018). Extraction of a photovoltaic cell's double-diode model parameters from data sheet values. Energy Science & Engineering, 6(5), 424-436. https://doi.org/10.1002/ese3.216.

[4] Charles, J.P. et al. (1985). Consistency of the double exponential model with physical mechanisms of conduction for a solar cell under illumination. J. Phys. D: Appl. Phys. 18 226.

[5] Ezike S. et al. (2023). Extraction of five photovoltaic parameters of nature-based dye sensitized solar cells using single diode model. Renewable Energy Research and Applications, Vol. 4, No. 2, pp 199-208.

[6] Xiao W., Lind M.G., Dunford W.G., and Capel A. (2006). Real-time identification of optimal operating points in photovoltaic power systems. IEEE Transactions on Industrial Electronics 53 (4), pp 1017–1026.

[7] Chen Y. et al. (2011). Parameters extraction from commercial solar cells I-V characteristics and shunt analysis. Applied Energy, Vol. 88, No. 6, pp 2239–2244.

[8] Shaheen, A. and Ginidi, A. (2023). Electrical parameters extraction of PV modules using artificial hummingbird optimizer. Scientific Reports, 13(1), 1-23. https://doi.org/10.1038/s41598-023-36284-0.

[9] Ortiz-Conde A., Sánchez F.J.G., and Muci J. (2006). New method to extract the model parameters of solar cells from the explicit analytic solutions of their illuminated I-V characteristics. Solar Energy Materials and Solar Cells, Vol. 90 (3), pp. 352–361.

[10] Cubas, J., Pindado, S., and Victoria, M. (2014). On the analytical approach for modeling photovoltaic systems behavior. Journal of Power Sources, 247, 467-474.

[11] Tamrakar, R. and Gupta, A. (2015). A review: extraction of solar cell modelling parameters. International journal of innovative research in electrical, electronics, instrumentation and control engineering, Vol. 3, No.1, pp. 55–60.

[12] Jain, A. and Kapoor, A. (2005). Exact analytical solutions of the parameters of real solar cells using Lambert W-function. Solar Energy Materials and Solar Cells, Vol. 85, pp 391–396.

[13] Jain, A., Sharma, S., and Kapoor, A. (2006). Solar cell array parameters using Lambert W-function. Solar Energy Materials and Solar Cells, Vol. 90, pp. 25-31.

[14] Nguyen H. et al. (2022). Solar PV Modeling with Lambert W Function: An Exponential Cone Programming Approach. IEEE Kansas Power and

Energy Conference (KPEC), Manhattan, KS, USA, 2022.

[15] Nassar-eddine I. et al. (2016). Parameter estimation of photovoltaic modules using iterative method and the Lambert W function: A comparative study, Energy conversion and Management, Vol. 119, pp. 37-48.

[16] Gao, X.-K & Yao, C.-A & Gao, Xiankun & Yu, Y.-C. (2014). Accuracy comparison between implicit and explicit single-diode models of photovoltaic cells and modules. Wuli Xuebao/Acta Physica Sinica. 63. 10.7498/aps.63.178401.

[17] Jinlei, D. and Radhakrishnan, R. (2008). A new method to determine the optimum load of a real solar cell using the Lambert W-function. Solar Energy Material and Solar Cells, Vol. 92, No. 12, pp. 1566–1569.

[18] Peng L. et al. (2013). A new method for determining the characteristics of solar cells. Journal of Power Sources, Vol. 227, pp. 131–136.

[19] Cubas, J., Pindado, S., and De Manuel C. (2014). Explicit Expressions for Solar Panel Equivalent Circuit Parameters based on Analytical Formulation and the Lambert W-Function. Energies. Vol. 7(7), pp 4098-4115. https://doi.org/10.3390/en7074098.

[20] Tripathy, M., Kumar, M., and Sadhu, P.K. (2017). Photovoltaic system using Lambert W function-based technique. Solar Energy, Vol. 158, pp. 432-439.

[21] Li J. et al. (2023). Extraction of Single Diode Model Parameters of Solar Cells and PV Modules by Combining an Intelligent Optimization Algorithm with Simplified Explicit Equation based on Lambert W Function. Energies, Vol. 16, No. 14, 5425.

[22] Maghami, M.R. et al. (2016). Power loss due to soiling on solar panel: A review. Renewable and Sustainable Energy Reviews, Vol. 59, pp. 1307-1316.

[23] Patel, H. and Agarwal, V. (2008). MATLAB-based modelling to study the effects of partial shading on PV array characteristics. IEEE Trans. on Energy Conversion. 23 (1), 302-310.

[24] Martinez-Moreno, F. et al. (2010). Experimental model to estimate shading losses on PV arrays. Solar Energy Materials and Solar Cells, Vol. 94, pp. 2298-2303.

[25] Paraskevadaki, E.V. and Papathanassiou, S.A. (2011). Evaluation of MPP voltage and power of mc-Si PV modules in partial shading conditions. IEEE Transactions on Energy Conversion, Vol. 26, pp. 923-932.

[26] Bastidas J. D. et al. (2013). A model of photovoltaic fields in mismatching conditions featuring and improve calculation speed. Electric Power Systems Research, Vol. 96, pp. 81-90.

[27] Batzelis, E.I. and Routsolias, I.A. (2014). An explicit PV string model based on Lambert W function and simplified MPP expressions for operation under partial shading. IEEE transactions on Sustainable energy, Vol. 5, No. 1, pp. 301-312.

[28] Fathabadi, H. (2015). Lambert W function based technique for tracking the maximum power point of PV modules connected in various configuration. Renewable Energy, Vol. 74, pp. 214-226.

[29] Argawal, N. and Kapoor, A. (2018). Investigation of the effect of partial shading on series and parallel connected solar photovoltaic modules using Lambert W-function. AIP Conf. Proc.2006,030050-1-030050-5; https://doi.org/10.1063/1.5051306.

[30] Pendem, S.R. and Mikkili, S. (2018). Modelling and performance assessment of PV array topologies under partial shading conditions to mitigate the mismatching power losses. Solar Energy, Vol. 160, pp. 303-321.

[31] Prince Winston D. et al. (2020). Performance improvement of solar PV array topologies during various partial shading conditions. Solar Energy, Vol. 196, pp. 228–242.

[32] Bingöl, O. and Özkaya, B. (2018). Analysis and comparison of different PV array configurations under partial shading conditions. Solar Energy, Vol. 160, pp. 336–343.

[33] Kaushika, N.D. and Gautam, N.K. (2003). Energy yield simulations of interconnected solar PV arrays. IEEE Transactions on Energy Conversion, Vol. 18, No. 1, pp. 127-133.

[34] Hsu, Y.J. and Hsu, P.C. (2011). An investigation on partial shading of PV modules with different connection configurations of PV cells. Energy, Vol. 36, pp. 3069–3078.

[35] Ramaprabha, R. and Mathur, B.L. (2012). A comprehensive review and analysis of solar photovoltaic array configurations under partial shaded condition. International Journal of Photoenergy. 2012, pp 1-17.

[36] Osmani K. et al. (2022). Mitigating the effects of partial shading on PV system's performance through PV array reconfiguration: A review. Thermal Science and Engineering Progress, Vol. 31, 101280.

[37] Rezazadeh S. et al. (2022). Photovoltaic array reconfiguration under partial shading conditions for maximum power extraction: A state-of-the-art review and new solution method. Energy Conversion and Management, Vol. 258, 115468.

[38] Gao X. et al. (2023) Divide and Conquer Q-Learning (DCQL) algorithm based Photovoltaic (PV) array reconfiguration scheme for alleviating the partial shading influence, Solar Energy, Volume 249, pp. 21-39.

[39] Solis-Cisneros H. I. et al. (2022). A dynamic reconfiguration method based on neuro-fuzzy control algorithm for partially shaded PV arrays. Sustainable

Energy Technologies and Assessments, Volume 52, Part B, 102147, ISSN 2213-1388.

[40] Sagar G. et al. (2020). A Su Do Ku puzzle based shade dispersion for maximum power enhancement of partially shaded hybrid bridge-link-total-cross-tied PV array. Solar Energy, Vol. 204, pp. 161–180, doi: 10.1016/j.solener.2020.04.054.

[41] Agrawal N. et al. (2021). Performance Enhancement by Novel Hybrid PV Array Without and With By-pass Diode Under Partial Shaded Conditions: An Experimental Study. International journal of renewable energy research, Vol. 11, No. 4, pp 1881-1891.

[42] Agrawal, N., Bora, B., and Kapoor, A. (2020). Experimental investigations of fault tolerance due to shading in photovoltaic modules with different interconnected solar cell networks. Solar Energy, Vol. 211, pp. 1239-1254.

[43] Bana, S. and Saini, R.P. (2017). Experimental investigation on power output of different photovoltaic array configurations under uniform and partial shading scenarios. Energy, Vol. 127, pp. 438–453.

[44] Drif, M. et al. (2012). A comprehensive method for estimating energy losses due to shading of GC-BIPV systems using monitoring data. Solar Energy, Vol. 86, No. 9, pp. 2397–2404.

[45] Saber, S. E. et al. (2014). PV (photovoltaics) performance evaluation and simulation-based energy yield prediction for tropical buildings. Energy, Vol. 71, pp. 588–595. doi: 10.1016/j.energy.2014.04.115.